

Author

Alexander Kamptner

Submission

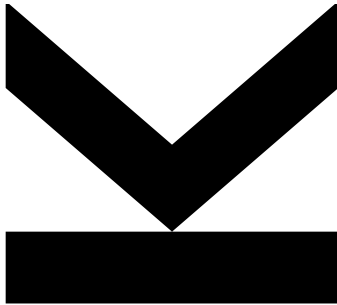
**Institute of Physical
Chemistry and Linz
Institute for Organic
Solar Cells**

Thesis Supervisor

**a. Univ. Prof. Dr.
Markus Scharber and
apl.-Prof. Dr. Manuela
Schiek**

October 2023

Ellipsometry on Organic Semiconductors



Bachelor's Thesis

to obtain the academic degree of

Bachelor of Science

in the Bachelor's Program

Technische Physik

Contents

Abstract	i
1 Introduction	1
2 Physical Background	3
2.1 General Physical Background	3
2.2 Ellipsometry	6
2.2.1 Standard Ellipsometry	8
3 Methods and Experiments	11
3.1 Introduction of the Analyzed Polymers	11
3.2 Sample Preparation	13
3.2.1 Glass Substrate	13
3.2.2 Polymer Solution	15
3.2.3 Doctor Blading	15
3.3 Ellipsometry	17
3.3.1 Standard Ellipsometry in Reflection	17
3.3.2 Transmission Intensity	19
3.4 Profilometry	20
4 Evaluation of the Ellipsometry Data	21
4.1 Glass Substrate Layer and General Evaluation Process	22
4.2 Polymer Layer	24
4.3 Evaluated Measurements	27
4.4 Results	29
4.4.1 Thicknesses	29
4.4.2 Complex Refractive Indices	32
5 Absorption Coefficient and Energy Gap	33
5.1 Absorption Coefficient	33
5.2 Tauc Plot and Energy Gap	36
6 Summary	40
List of Figures	42
List of Tables	42
References	43

Abstract

This thesis discusses the optical properties of organic semiconductors. The aim is to determine the anisotropic complex refractive index, the absorption coefficient and the energy gap of several organic semiconductors and the relation of the absorption coefficient and the energy gap. Six polymers were analyzed, which were deposited as a thin film on a glass substrate. Ellipsometry was used to determine the optical constants of the polymers and the thickness of the layers, and with a profilometer the thickness was measured again, to compare both results. Then the anisotropic complex refractive index was needed to calculate the absorption coefficient, which was used to calculate the Tauc Plot. Afterwards the energy gap of each polymer was calculated with the Tauc Plot method. Finally, the first peak with the lowest energy of the absorption coefficient was plotted as a function of the energy, and separately, as a function of the energy gap.

1 Introduction

Solar cells already make a significant contribution to energy supply today. In the coming years, this share is expected to increase even further. Solar cells are not only used for electricity grid power supply but also in devices like pocket calculators and other small devices. However, the list of applications extends further, with satellites being powered by solar cells. In many of these applications, solar cells made from inorganic semiconductors, such as silicon, are commonly used. Nevertheless, there is also the possibility to construct solar cells from organic materials. While inorganic solar cells generally exhibit higher efficiency and better temperature stability than organic ones, the latter have several other advantages. Organic solar cells, for instance, are more cost-effective to manufacture and relatively thin, making them exceptionally lightweight. Furthermore, due to their essentially plastic nature, they are flexible and easy to handle. [13]

The major topic being discussed here however, is a bit different. In general, solar cells should be able to capture a large portion of the solar spectrum, meaning absorbing as much as possible, to minimize unused incoming solar energy. This requires the ability to capture and convert a wide range of photons, from the far infrared to the far ultraviolet spectrum, into electrical energy. Therefore, the minimum energy required for photon absorption should be low, meaning the energy gap should be small. Additionally, solar cells should ideally be thin to conserve materials, thereby reducing cost and weight. However, this is where the issue with inorganic solar cells arises: the smaller the minimum absorbable energy, meaning the smaller the energy gap, the lower the absorption coefficient (of the first peak). This is referred to as the “energy gap law.” [1] This relationship is well-established and confirmed for inorganic semiconductors, but not for organic ones. Therefore, the examination of this behavior, i.e. the relation between the energy gap and the first maximum of absorption coefficient, of selected organic semiconductors, is the subject of this bachelor’s thesis.

To accomplish this, a set of organic semiconductors is chosen, each with an approximately known energy gap, that spans a broad range of the energy spectrum. The organic semiconductors are then deposited as a thin film on a glass substrate. From these polymers, the absorption coefficient and the energy gap will then be determined. To accomplish this, the complex refractive index must be derived, using a technique known as ellipsometry. In ellipsometry, the reflection and transmission properties of the semiconductors are measured, providing the data needed to determine the complex refractive index. This is achieved by simulating the behavior of the measured sample within a program and then fitting the simulation to the observed characteristics. The simulated model can subsequently be utilized to ascertain the complex refractive index. Furthermore, the program provides an estimation of the sample's thickness. This data can be compared with results obtained through an alternative thickness determination technique, which in this case will be profilometry. Then the imaginary part is employed for calculating the absorption coefficient. Subsequently, the Tauc plot method is applied to calculate the energy gap. In the final step, the first maximum at the lowest energy of the absorption coefficient, is plotted as a function of its location at the energy spectrum, and as a function of the calculated energy gap.

2 Physical Background

2.1 General Physical Background

Light

Light is an electromagnetic and transverse wave. An interesting part of light is the one, that has a wavelength between about 400 to 800 nm , which is approximately the visible spectrum. However, here the term light is used for the wider range from about 200 nm to 1600 nm . As light is a transverse wave, it has three possible polarizations: linear, circular and elliptical, which is a combination of the two before.

When light passes through a medium, it may change its speed, and additionally a part of it can be absorbed. This phenomenon can be described by the complex refractive index:

$$(n + ik)(\lambda) \quad (2.1)$$

Where n is the real part, often simply called refractive index, and k is the imaginary part. In general, both are called optical constants and are wavelength-dependent (and therefore frequency-dependent), so the complex refractive index is wavelength-dependent as well.

The refractive index n describes the relation between the speed of light in vacuum, which is a natural constant, and the one in the material:

$$n(\lambda) = \frac{c_0}{c_M(\lambda)} \quad (2.2)$$

Where n is the refractive index, c_0 is the speed of light in vacuum and c_M is the speed in the medium.

The imaginary part of the complex refractive index is called extinction coefficient k and is related to the absorption. It is used to calculate the absorption coefficient α by the following formula:

$$\alpha = \frac{4\pi k}{\lambda} \quad (2.3)$$

Energy gap

The bandgap, also called energy gap, is a term used in solid states physics and describes an amount of energy. In the ground state, the electrons of a solid occupy the lowest possible states, with the highest one being the valence band. The next highest possible state is the conduction band. The energy difference between those two bands is called “bandgap” (See Figure 2.1) and can be used to classify materials: conductors (or metals) have a very small or no bandgap (this means the two bands are either touching or overlapping), semiconductors have a small one and insulators have a large bandgap.

In organic semiconductors the equivalent to the bandgap is the HOMO/LUMO gap (See Figure 2.2) hereinafter referred to as energy gap, but the principle is very similar: in the ground state the electrons occupy the lowest possible molecular orbitals with the highest one being the HOMO (abbreviation of highest occupied molecular orbital). The next highest orbital is the LUMO (Lowest unoccupied molecular orbital). If an incoming photon should excite an electron to a higher orbital, it requires a minimum amount of energy (the HOMO/LUMO energy gap) to jump from the HOMO to the LUMO. Photons of higher energy may excite the electron to an even higher orbital, but photons of a lower energy are unable to excite any electrons.

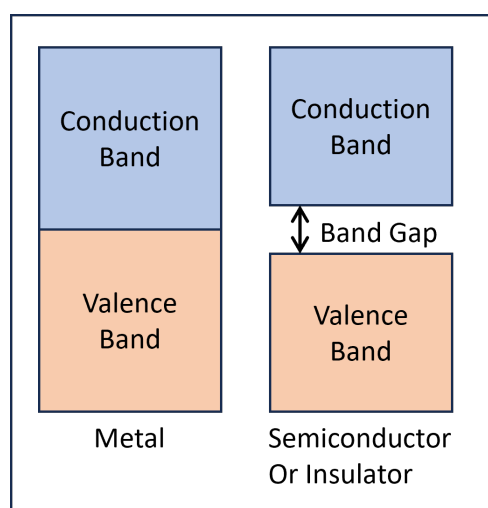


Figure 2.1: Bandgap Explanation

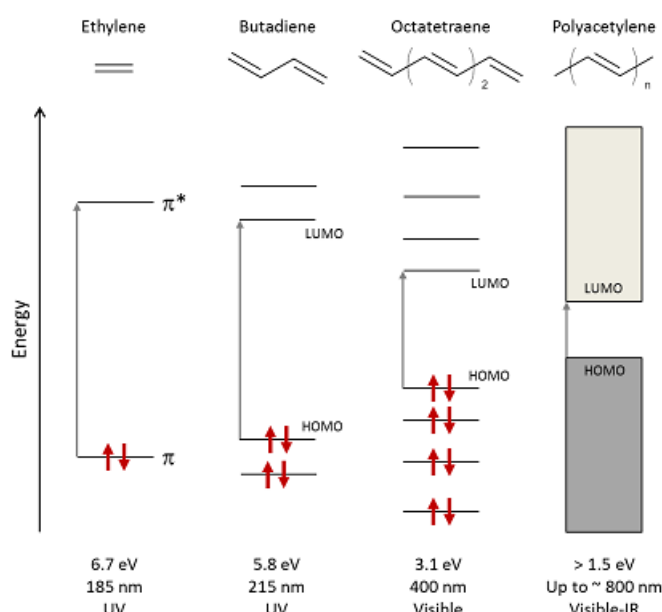


Figure 2.2: HOMO/LUMO gap [14]

Anisotropy

In general, anisotropy is the term for the direction dependency of a property. Here only uniaxial anisotropy is important. This means, that the complex refractive index of one direction (the z -direction) is different to the other two directions (x -direction and y -direction). The ray that is oscillating along the z -axis is called extraordinary ray, while the two other rays, along the x -axis and y -axis are called ordinary rays.

The following Figure (2.3) shows an example. A light beam travels through an anisotropic medium in the direction y , so its electric field oscillates in both directions, the ordinary (x) and the extraordinary one (z), and can be separated in those two components (E_x and E_z). In this example, the refractive index n of the x -direction is similar to the surrounding medium, and the extinction coefficient k is zero. So the ordinary part of the complex refractive index of the anisotropic medium is equal to the surrounding medium and the E_x component travels through it unaffected. Whereas the E_z component (the extraordinary ray) gets attenuated and travels with reduced speed, resulting in a smaller wavelength. After traveling through the anisotropic material, the two components are, in general, phase shifted and not necessarily the same size anymore.

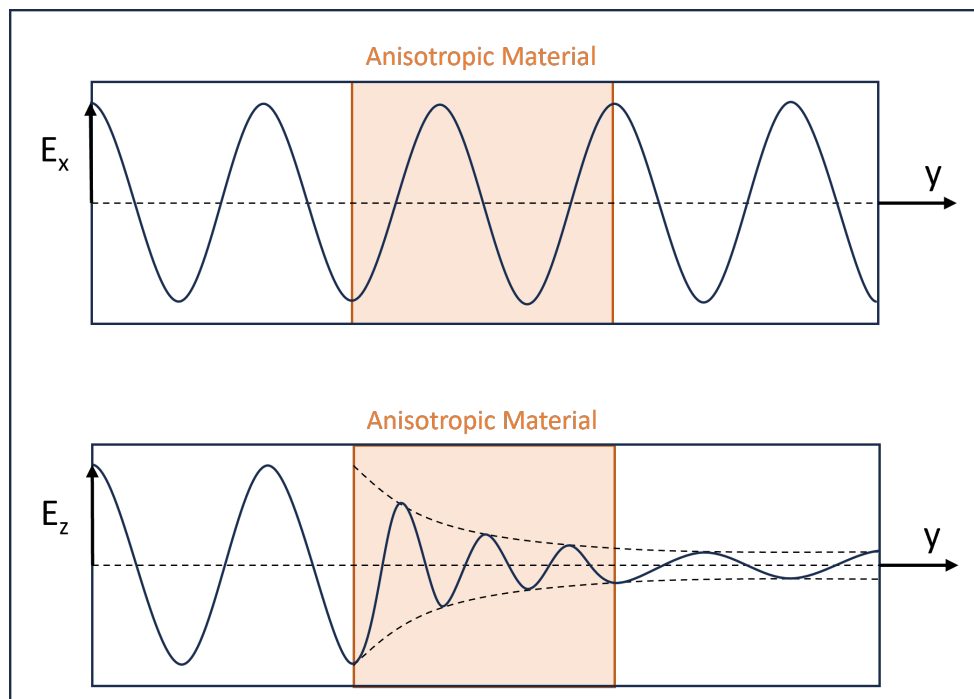


Figure 2.3: Effect of Anisotropy: The two perpendicular components E_x and E_z of the electric field of a light beam are both propagating along the y -axis, but influenced differently when traveling through the anisotropic material

2.2 Ellipsometry

There are several different interactions of light and material. However, the following three are the most important here:

1. reflection
2. absorption
3. transmission

The law of reflection states that when a ray of light reflects off a surface, the angle of incidence θ_i is equal to the angle of reflection θ_r . These two beams span the plane of incidence seen in Figure 2.4. This plane is important for the consideration of the s-polarized and p-polarized parts of the light. The s-polarized (s for the German word “senkrecht”, which means perpendicular) part is the one, where the electric field oscillates perpendicular to the plane of incidence. The electric field of the p-polarized part oscillates parallel to this plane.

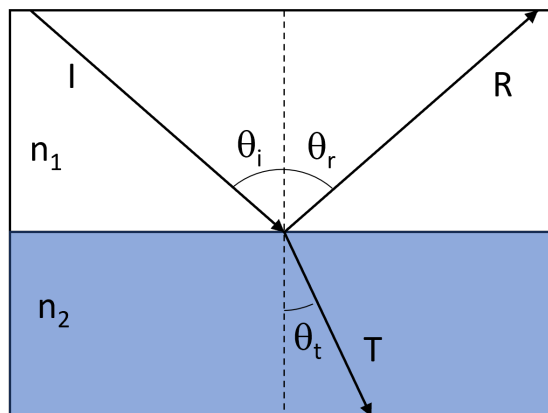


Figure 2.4: Angle of Incidence: The incoming (I), the reflected (R) and the transmitted (T) ray and their angles are shown

Reflection occurs at every interface between two materials of different refractive indices. The amount of both, the reflected and transmitted light can be calculated by the Fresnel equations. The two Fresnel equations for the electric field of the reflected beam are shown in equations (2.4).

The reflectance for the s-polarized light is

$$r_s = \frac{n_1 \cos(\theta_i) - n_2 \cos(\theta_t)}{n_1 \cos(\theta_i) + n_2 \cos(\theta_t)} \quad (2.4a)$$

while the reflectance for the p-polarized light is

$$r_p = \frac{n_1 \cos(\theta_t) - n_2 \cos(\theta_i)}{n_1 \cos(\theta_t) + n_2 \cos(\theta_i)} \quad (2.4b)$$

Where n_1 and n_2 are the refractive indices of the media, and θ_i and θ_t are the incoming and transmitted rays respectively.

The non-reflected part then travels through the material and can be absorbed there, if the photon can excite a particle of the right oscillation frequency. If there is a part of the light remaining, it reaches the next interface of two materials with different refractive indices and can here be reflected again, or transmitted and leaves the material.

All those interactions are related as it can be seen in equation (2.5).

$$T = 1 - R - A - S \quad (2.5)$$

Where T (Transmission), A (Absorption) and S (Scattering) stand for the ratio of the incoming light intensity. Scattering is mentioned in this equation for the general case, however it only occurs at rough layers and therefore does not occur in a significant amount in this thesis.

Although the attenuation coefficient, and therefore the absorption-interaction, is one of the main information to be determined in this thesis, the ellipsometer can only measure the reflected and transmitted light. The information about the optical constants and therefore the attenuation coefficient, can only be determined after the experiment, by evaluating the measurement data with a program (Complete Ease V6), that will be explained later.

2.2.1 Standard Ellipsometry

The ellipsometer uses polarized light of a wide frequency range. The polarization of the light can either be linear or circular. The one, that was used for the measurement here uses linear polarized light of a wide wavelength range, produced by a xenon lamp. The light travels through the air until it reaches the sample. The sample consists of a glass plate, which is the substrate, and on top of it is a thin film of the organic semiconductor. When the light of the ellipsometer reaches the first layer of the sample (the organic semiconductor), a part of it can be reflected and the rest gets transmitted to the second layer (the glass substrate), where it can be reflected and transmitted again (See Figure 2.5). While traveling through the media a part of the light can be absorbed. After the transmission through the whole sample, the light gets reflected or absorbed on the sample holder. In addition to the first reflection, the light, that is transmitted through the layer, but then reflected at the next interface (glass plate), travels back through the previous layers and there it can be reflected again at the interface of two layers. The reflection spectrum then travels again through the air and will be detected by the ellipsometer in the end. The detected spectrum is used to determine the optical constants by the computational tool.

The coherence length of the xenon lamp's light is in the order of magnitude of the wavelength, approximately 10 to 100 *nm*. While the thickness of the polymer layer is in this order too, the thickness of the glass substrate is too large (1 *mm*). Therefore, the light, that is reflected at the backside of the glass substrate is not coherent anymore, which must be taken into account, by adding the option "Include Depolarization Data" later in the Evaluation Chapter.

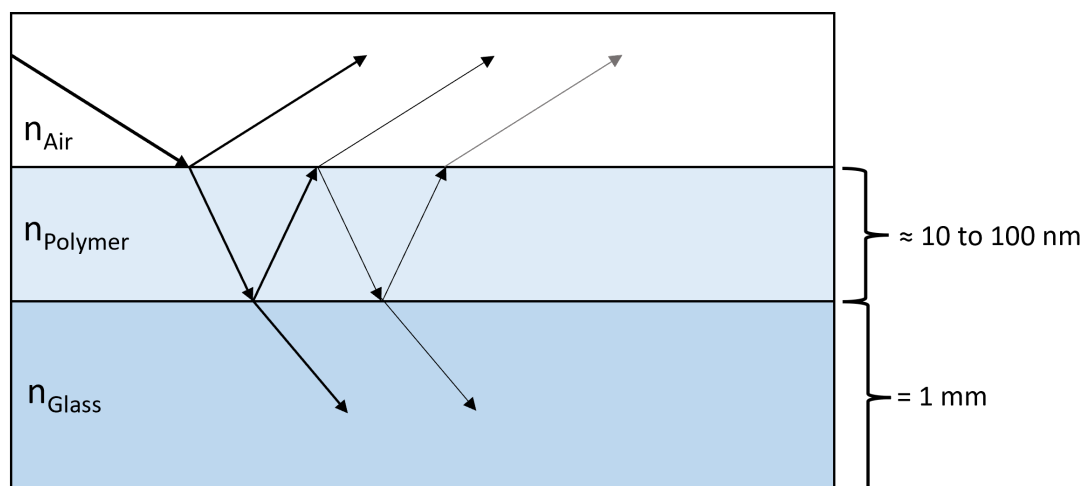


Figure 2.5: The incoming light ray gets reflected and transmitted at each interface. A part of it gets absorbed while traveling through the media.

The important information for ellipsometry is now the polarization of the reflected light. Before the interaction with matter, the light was polarized linearly, but is “rotated” to 45 degrees. So this linear polarized light can be separated into two components of equal amplitude, one in the x-direction and one in the z-direction. The one in the x-direction is the so called s-polarized light and the one in the z-direction is the p-polarized light.

Since these two components are reflected differently (in terms of intensity and phase shift) the total reflected beam is not polarized linearly anymore. In fact, this reflected beam has the shape of an ellipse, hence the name ellipsometry. There are now two phase shifts, that are used to evaluate the optical constants, which are called the Ψ and Δ shifts and their relation to the reflectances r_s and r_p is shown in equation 2.6. Ψ is the “new tilt angle” of the now just partially polarized light, or in other words, Ψ is the proportion between the s-polarized and the p-polarized part (See Figure 2.6). Δ is the “thickness” of this ellipse, or more precise the time difference between the s-polarized part and the p-polarized part (See Figure 2.7). Since in this measurement only the relation between these two polarized components is measured, it is not required to initialize the intensity from the xenon lamp.

$$\rho = \tan(\Psi) \cdot e^{i\Delta} = \frac{r_p}{r_s} \quad (2.6)$$

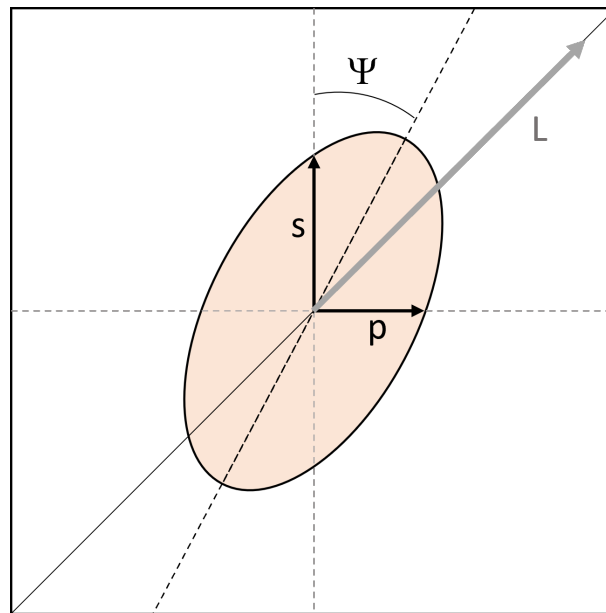


Figure 2.6: The s-polarized (s) and p-polarized part (p) of the reflected beam cause the tilt Ψ . The incoming light beam (L) was linearly polarized

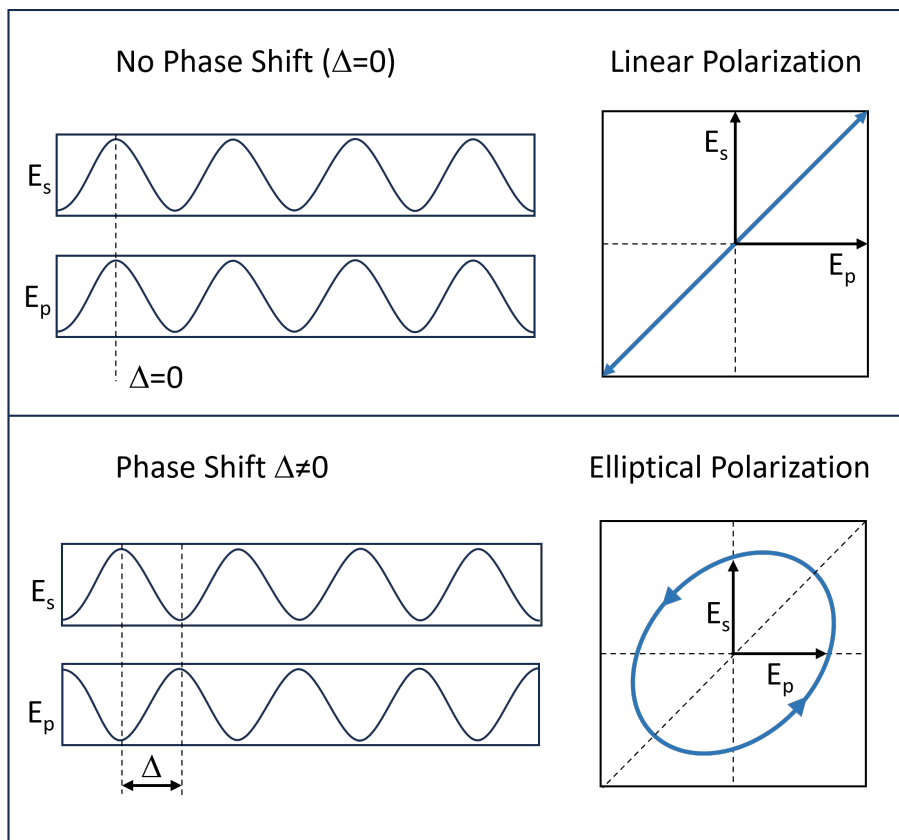


Figure 2.7: When the light is linearly polarized, the s-component and the p-component are in phase ($\Delta = 0$). Once the beam gets reflected, the two polarization components are out of phase (phase shift Δ), causing an elliptical polarization.

3 Methods and Experiments

3.1 Introduction of the Analyzed Polymers

There were six polymers analyzed, produced in five series. The series numbers, a short description of the polymer, their full name and the molecular formula are shown below. The structural formula is presented as an image on the right side.

F8BT

Series: 1,2

Full Name: Poly(9,9-dioctylfluorene-alt-benzothiadiazole)

Molecular Formula: $(C_{35}H_{42}N_2S)_n$

This Polymer is also called PFBT and is used for instance, for green OLEDs, OFETs and light emitting transistors. [5]

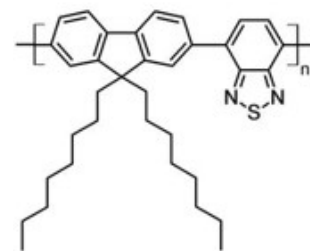


Figure 3.1: F8BT

MDMO-PPV

Series: 4

Full Name: Poly-[5-(3',7'-dimethyloctyloxy)-2-methoxy-1,4-phenylvinyl]

Molecular Formula: $(C_{19}H_{28}O_2)_n$

MDMO-PPV can be used as a red-light emitting polymer and in the fabrication of bulk heterojunction solar cells. [11]

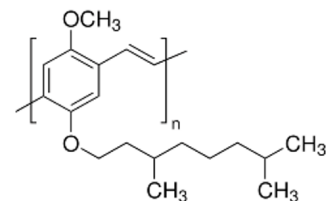


Figure 3.2: MDMO-PPV

PDCBT

Series: 1,2,3

Full Name:

Poly[2,2''-bis[[[(2-butyloctyl)oxy]carbonyl][2,2':5',2'':5'',2'''-quaterthiophene] -5,5''-diyl]

Molecular Formula: $(C_{42}H_{56}O_4S_4)_n$

The Polymer PDCBT is a medium-to-wide bandgap polymer and has been used in highly efficient fullerene free polymer cells. [8]

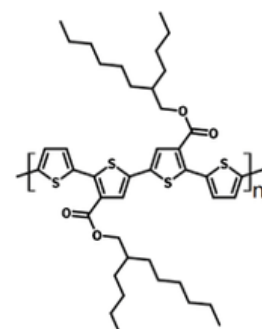


Figure 3.3: PDCBT

PTB7

Series: 1,4

Full Name: Poly [[4,8-bis[(2-ethylhexyl)oxy]benzo[1,2-b:4,5-b']dithiophene-2,6-diyl][3-fluoro-2-[(2-ethylhexyl)carbonyl]thieno[3,4-b]thiophenediyl]]

Molecular Formula: $(C_{41}H_{53}FO_4S_4)_n$

This polymer is used for polymer:fullerene solar cells and has a high solubility in a wide range of solvents. [9]

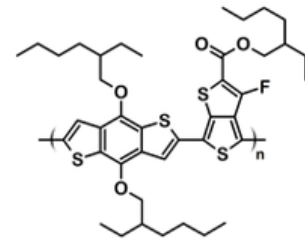


Figure 3.4: PTB7

PBDB-T-2F

Series: 3,4

Full Name: Poly[(2,6-(4,8-bis(5-(2-ethylhexyl-3-fluoro)thiophen-2-yl)-benzo[1,2-b:4,5-b']dithiophene))-alt-(5,5-(1',3'-di-2-thienyl-5',7'-bis(2-ethylhexyl)benzo[1',2'-c:4',5'-c']dithiophene-4,8-dione)]

Molecular Formula: $(C_{68}H_{76}F_2O_2S_8)_n$

PBDB-T-2F, also known as PBDB-T-F, PBDB-TF and PM6, is a medium bandgap polymer and is used in organic photovoltaics as the donor and ITIC-2F as the acceptor. [6]

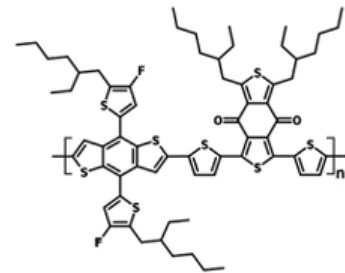


Figure 3.5: PBDB-T-2F

ZZ50

Series: 0,2

Full Name: Poly[2,6-(4,4-bis-(2-ethylhexyl)-4H-cyclopenta[2,1-b;3,4-b']dithiophene)-alt-4,7(2,1,3-benzothiadiazole)]

Molecular Formula: $(C_{31}H_{38}N_2S_3)_n$

ZZ50, also called PCPDTBT, is a low bandgap polymer semiconductor and, for instance, used for organic solar cells and OFETs. [7]

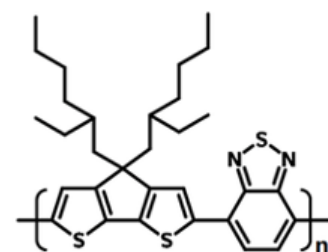


Figure 3.6: ZZ50

3.2 Sample Preparation

3.2.1 Glass Substrate

The actual part of the sample, that should be measured is the organic semiconductor. Since the organic semiconductor cannot be manufactured and therefore not be measured on its own, it has to get deposited on a substrate as a thin layer. The substrate that is used, is a microscope slide manufactured by Marienfeld and will be called “glass substrate” here. The size of the glass substrate is:

- length: 76 *mm*
- width: 26 *mm*
- thickness: 1 *mm*

Determining the Air Side

As this glass substrate is manufactured with the float glass technique, it has a “tin side” and an “air side”. Since the substrate has a different complex refractive index when its flipped from one side to the other, it is important, that only one specific side is used to deposit the organic semiconductor layer. The chosen side is the air side. It is not possible to determine a difference between the two glass substrate’s sides just by looking at it with the naked eye, so some of the blank substrates were measured randomly with the ellipsometer on both sides and the complex refractive indices were determined, see Figure 3.7.

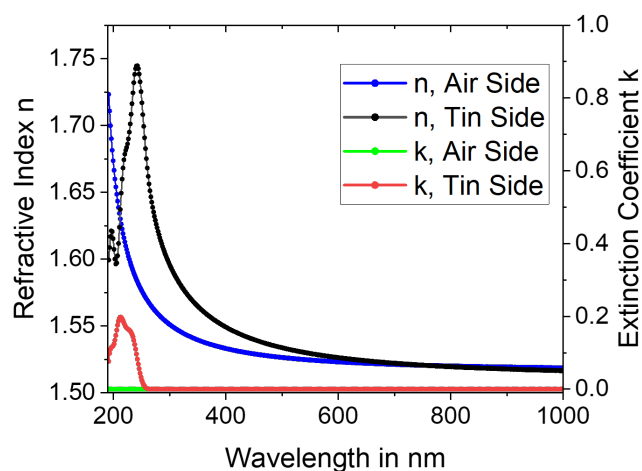


Figure 3.7: Complex Refractive Indices of Both Sides of the Glass

After some tests, there was enough evidence to show that all substrates were orientated in the same way in the box, so all substrates were labeled on the same side, the air side, to constantly recognize it.

Cleaning Process

Before the thin film can be deposited on the glass substrate, the substrate has to be prepared for the process. At first it has to be cleaned. To do so, the substrates are getting placed in a beaker and filled with a cleaning agent afterwards. Then the beaker, with the samples and the liquid in it, is put in the ultrasound machine and treated for 15 minutes. This procedure has to be applied for all three cleaning agents in the following order:

1. acetone
2. isopropanol
3. deionised water

After the ultrasound cleaning process is finished, the substrates were dried with a nitrogen gun.

The last step of the sample preparation is to activate the surface. The surface activation is required, so that the solution that will be put on the surface, is able to disperse homogeneously. This principle works as follows: If the surface energy is very low, the solution would rather form droplets on the substrate's surface than spreading out homogeneously. But if the surface energy is quite high, the solution tends to minimize the total energy of the system, by covering the whole surface homogeneously.

To activate the surface, and therefore to maximize its energy, the substrates were put into a plasma oven, and get etched in an oxygen atmosphere for 5 minutes at 100 Watts. After this last step of the preparation, the substrates can be used for depositing the polymers on them. It is important, that this last step has to be done just before the next step (doctor blading), because the surface is only activated for about 20 minutes after the plasma oven finished its cycle.

3.2.2 Polymer Solution

All Polymers were dissolved in chlorobenzene. The polymer ZZ50 had a concentration of 6 mg/ml, whereas all other polymers had a concentration of 5 mg/ml. The solutions were stored on a stirring panel at a temperature of approximately 80°C.

3.2.3 Doctor Blading

The process to manufacture the samples is called doctor blading, or blade coating. In this process the plasma-activated substrates were placed onto a table, heated to 80°C. The blade is placed above the substrate at a small distance of less than 1 *mm*. Then the solution is placed in the gap between the blade and the substrate, and being held there by capillary force. Now the blade is moved above the substrate with a constant speed. During the movement, most of the solution stays inside the gap between the blade and the substrate, but a small amount covers the surface, that is left behind by the moving blade. Before the blade reaches the end of the substrate, the movement has to be stopped and the remaining solution, that stayed inside the gap has to be removed. During this manufacturing process, or a few seconds afterwards, the polymers have to crystallize on the surface homogeneously and most of the solvent has to evaporate. Otherwise the thin film will be inhomogeneous and therefore cannot be used for the measurements. In general, the faster the blade and therefore the “solution gap” moves above the substrate, the thicker these polymer films get. However, the thickness has poor reproducibility [10] and therefore two samples that were produced with the same blading speed do not necessarily need to exhibit similar thickness. The slowest blading speed was 2.5 *mm/s*, the remaining ones were between 5 *mm/s* and 40 *mm/s*, with 5 *mm/s* steps.

At the end of each doctor blading process the samples were removed from the heating table and marked with the polymer name and their blading speed (See Figure 3.8). All samples had a covered glass area of approximately 2.5 x 5.5 *cm* and were stored in a sample holder and put in a glove box until the ellipsometry measurement is done.

Sample Batches

At least three samples of each polymer were produced, and most of the polymers were produced in at least two series, as it can be seen in the following list:

- **F8BT**: contains 6 samples, produced in 2 series: the 1st series (with blading speeds: 2.5 mm/s, 5 mm/s and 10 mm/s) and the 2nd one (10 mm/s, 20 mm/s and 30 mm/s)
- **MDMO-PPV**: contains 3 samples, produced only in the 4th series (5 mm/s, 10 mm/s and 15 mm/s)
- **PDCBT**: contains 8 samples, produced in 3 series: the 1st one (2.5 mm/s, 5 mm/s and 10 mm/s) the 2nd one (10 mm/s, 20 mm/s and 30 mm/s) and the 3rd one (10 mm/s and 20 mm/s)
- **PTB7**: contains 7 samples, produced in 2 series: the 1st one (2.5 mm/s, 5 mm/s and 10 mm/s) and the 4th one (10 mm/s, 15 mm/s, 25 mm/s and 35 mm/s)
- **PBDB-T-2F**: contains 4 samples, all of them were produced in the 4th series (10 mm/s, 15 mm/s, 20 mm/s and 30 mm/s)
- **ZZ50**: contains 6 samples, produced in 2 series: the 0 one (2.5 mm/s, 5 mm/s and 10 mm/s) and the 2nd one (10 mm/s, 20 mm/s and 40 mm/s)

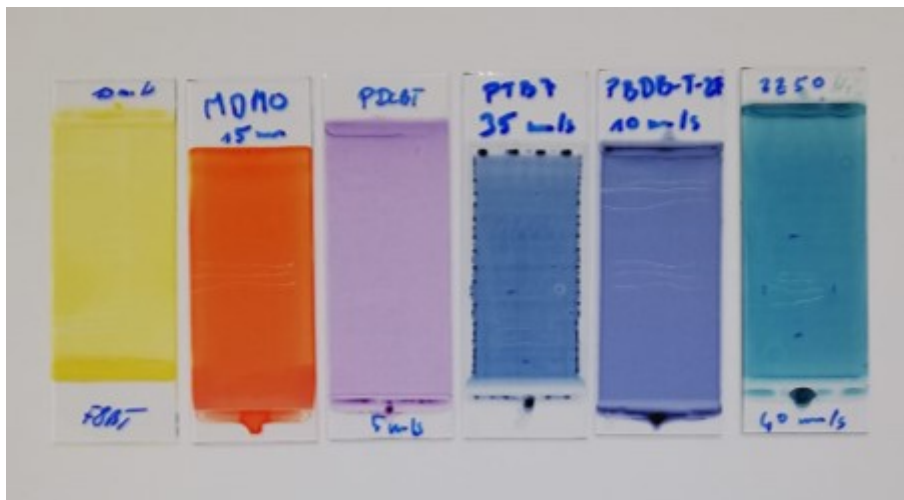


Figure 3.8: Some Labeled Samples of Each Polymer with Different Blading Speeds

3.3 Ellipsometry

There are two different measurement modes of ellipsometry used in this thesis. The first one is the standard ellipsometry, which measures the reflected light, when the incoming θ_i and also the reflected θ_r light beam has an angle of less than 90 degrees. The second one is the transmission intensity mode, where the incoming θ_i and transmitted θ_t beam are perpendicular to the sample surface. They are both shown in the following Sketch (Figure 3.9)

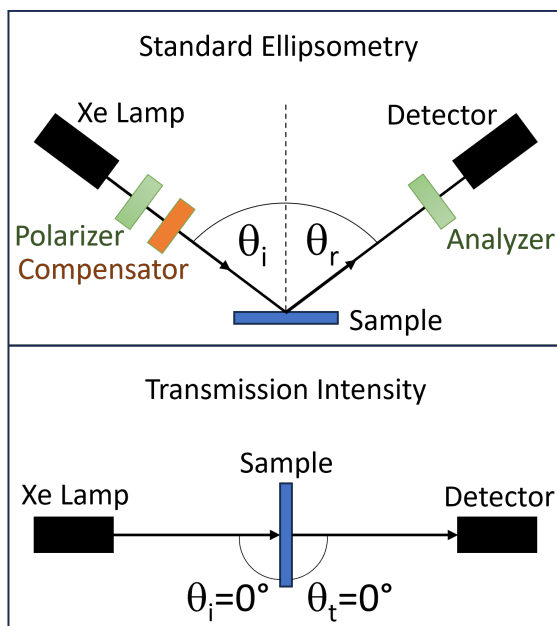


Figure 3.9: Ellipsometry Measurement Modes **Figure 3.10:** Ellipsometer Woollam M2000 [3]

3.3.1 Standard Ellipsometry in Reflection

After starting the ellipsometer (Woollam M2000 DI, See Figure 3.10) and the operating computer, the samples are placed on the sample holder, and the program to operate the ellipsometer (CompleteEase V5) should be opened. Before the first actual measurement, the detector apertures in the ellipsometer have to be adjusted, so that they receive as much intensity as possible, without an overload error in the program. For this purpose an initializing measurement has to be done, by using the transmission measurement mode. Both arms are positioned in a way, that the light beam points directly into the detector, so the arms are in a straight line. The sample must not be mounted in the light beam during this step, so it cannot disturb the initialization. Then the transmission measurement has to

be done with a live display of the current detected signal and the detector aperture has to be opened as far as possible. The UV-detector stays in the opened position, but the IR-detector's aperture will have to be closed a bit. Once the apertures are adjusted correctly, it can be found in the information on the program of the live displayed signal. If the program says that there is an overload, the aperture of the IR-detector has to be closed as far as mandatory, so the overload message disappears and therefore the detector is able to work as intended.

After this step, the samples can be measured in both modes. The first mode is the standard ellipsometry mode. The scanning angles were set to all angles between 45 and 75 degrees in 5-degree-steps. The sample thickness has to be set to 1 *mm* and the alignment angle to 55 degrees, which is the angle that is used in the following step.

After the software settings, the sample has to be aligned, so that the reflected light travels into the detector. The tilt alignment has to be adjusted manually, while the height alignment is done automatically by the machine directly before the actual measurement. To align the sample, the ellipsometer's arms are set to the so called alignment angle, and then the sample can be aligned by the adjusting screws. Before using these screws, it is required to check, if the reflected light beam is pointing at least near the detector. If that is the case, a small light dot that is located roughly at the detector's entrance, with a diameter of about 2 millimeters can be seen. Otherwise the adjustment screws have to be used to tilt the sample, thus moving the dot to the required location. For all following samples the rough adjustment should not be necessary anymore, unless the sample holder is changed, or the displayed signal is lost again.

The following fine adjustment is necessary before all standard ellipsometry measurements, even if the same sample is measured again, but placed differently. To do this fine alignment, the program displays the detector signal by dividing the detector into four equal parts. If all four parts receive the equal amount of intensity, the manual alignment is finished. This can be achieved by adjusting the screws of the sample holder in a way, that the displayed red cross of the program fits the gray one. Then the measurement can start, after the automatic height alignment of the ellipsometer.

Before measuring the actual sample, it is important to measure the glass substrate on it own, with the air side being orientated up. This is important, because the sample, that consists of the polymer layer and the glass substrate, will show the combined behavior of both materials. Once this measurement of only the glass substrate is done, it can later

be “subtracted” from the combined sample data, and therefore the characteristics of just the polymer layer can be determined. Before measuring both, the glass substrate and the sample, they have to be cleaned with the nitrogen gun.

After the measurement is finished, the program displays the measured data on an additional page. To check, if the measured sample has any anisotropic behavior, or an inhomogeneous film thickness, it is recommended to do at least a second measurement of the sample in a different orientation and on a different measured position. As mentioned before, the fine alignment has to be done again in this case. After another measurement, both can be compared by the command “Append Data”. If these two measurements do not fit (approximately), it is recommended to do enough other measurements, to determine those differences. Every measurement file was labeled with the name of the semiconductor, the doctor blading speed, and the measurement mode. The measurement modes are either standard ellipsometry (abbreviated by SE) or transmission intensity (abbreviated by T), in the file name.

3.3.2 Transmission Intensity

The second measurement mode, that is used to determine the optical constants, is the transmission intensity measurement. Here the sample is mounted in a way, that the light from the xenon lamp will be transmitted through it and reaches the detector. Therefore the initial intensity from the xenon lamp has to be determined before the actual measurement. To do so, the transmission measurement is divided into the following steps: At first the program instructs the user to remove the sample. The transmitted intensity will be measured without the mounted sample, to initialize the intensity which reaches the detector. Once the machine has finished the initialization step, the program informs the user to mount the sample since there is no automatic alignment in this mode.

The second part of the alignment is to place the sample perpendicular to the light beam, so that the light travels through the sample in the shortest way possible. To achieve this orientation, someone has to watch the reflection of the beam by standing right behind the detector arm and looking to the lamp arm. The reflection can be seen as a small dot again anywhere near the lamp arm. This dot should be directly at the aperture where the light beam leaves the lamp arm, so that the reflected light beam points exactly back into its origin.

When the sample alignment is finished, the measurement can be started. Once again it is displayed on the program page, but in this case it is not necessary to do another measurement, unless there was evidence of inhomogenous film thickness in the standard ellipsometry mode. If this is the case, then all positions that were measured in the first mode, should be measured again. It is not necessary to measure the additional position, if there was evidence of anisotropic behavior, since the transmission measurement is not affected by the planar anisotropy, but by the film thickness. It is again important, to measure not only the manufactured samples, but also the glass substrate on its own, for the same reason mentioned before.

3.4 Profilometry

The used profilometer is the Dektak XT that can measure the thickness of a thin film on a substrate. It employs a scanning needle with a diameter of 2 μm , which slides across the sample at a scanning speed of 100 μm per second. Therefore it can detect small steps on the surface of the measured object. Consequently, it is necessary to manually scratch the thin film with a needle, resulting in small stripes where the film is removed from the substrate, leaving unaffected regions where the film remains intact. This process is used to verify the accuracy of the ellipsometry results by comparing the thickness measurements.

4 Evaluation of the Ellipsometry Data

The measured data in ellipsometry are, as mentioned, the intensity relations between either two polarizations, like in standard ellipsometry, or the intensities before and after mounting the sample in the light beam, as in the transmission mode. Since the required data was not only the thickness but the optical constants of the organic semiconductor in particular, these data has to be evaluated by the software program called “Complete Ease”.

To evaluate the measurement data, the software has multiple options to build a model of the real sample and simulate the behavior. In addition to that, the program can modify the parameters of the model to fit the given measurement data to the calculated one as best as possible. If the model should fit the real sample even better, more parameters have to be added to the model, meaning the complexity of the model will increase. The quality of this fit is defined by the Mean Square Error, abbreviated by MSE. It is calculated by the average of all quadratic deviations of the given values and their corresponding calculated values, shown in formula (4.1).

$$MSE = \frac{1}{n} \cdot \sum_{i=1}^n (Y_i - \hat{Y}_i)^2 \quad (4.1)$$

Where n is the number of variables, Y_i is the observed value, and \hat{Y}_i is the predicted value.

Complete Ease uses this basic formula to calculate its MSE with formula (4.2), that can be found in the user manual [2].

$$MSE_{NCS} = \sqrt{\frac{1}{3n - m} \sum_{i=1}^n \left[\left(\frac{N_{E_i} - N_{G_i}}{.001} \right)^2 + \left(\frac{C_{E_i} - C_{G_i}}{.001} \right)^2 + \left(\frac{S_{E_i} - S_{G_i}}{.001} \right)^2 \right]} \quad (4.2)$$

Where n is the number of wavelengths, m is the number of fit parameters, and $N = \cos(2\Psi)$, $C = \sin(2\Psi)\cos(\Delta)$, $S = \sin(2\Psi)\sin(\Delta)$. The indices E stand for the measured data, while the G ones stand for the model generated data.

The MSE should be as low as possible, with a reasonable complexity of the model. This means, that every added fit parameter should decrease the MSE enough, to justify the increasing complexity of the model. As a guide value, it can be said that every added parameter should cause a decrease of the MSE to approximately 75 % of its previous value. Furthermore the target value of the MSE should be lower than 10, or even better, lower than 5. In this thesis, most of the MSE values accumulate in a range between 4 and 8.

If there are more samples with the same sample characteristics available, all these measured data should be evaluated at once. Same sample characteristics means, that all samples must have the same type of organic semiconductor as their polymer layer. In addition to that, all samples must have the same glass type with the same orientation as their substrate. That being the case, the systematic error can be decreased. Here, all samples of the same polymer and the same series but with different layer thicknesses, are combined in one evaluation. After the series-wise evaluation, there was a second one, where all samples of a specific polymer of all series were evaluated together.

4.1 Glass Substrate Layer and General Evaluation Process

The following steps are very similar to the evaluation of the polymer layer and therefore will be described just once and referred to later in the “Polymer Layer” section.

Loading the Files

The first step to receive the optical constants is to build a model of the measured sample in the software. Here it is important to mention, that the characteristics of the glass substrate influenced the measurement itself, but should not influence the resulting optical constants in the end. So, at first it is required to build a model for the glass substrate only. Before that, all measurement data of the substrate measurements alone, has to be loaded into the program. For the first file, it has to be done, by opening one of the measurement files, the remaining ones have to be appended. After this step every measurement file of one particular sample should have been loaded into the program.

Model Building and Presets

The first step to build the required model is to create a layer with Cauchy characteristics. This layer uses Cauchy's equation to first fit the transparent part of the layer. Cauchy's equation (4.3) describes the relation between the refractive index of a certain transparent medium and the wavelength of light.

$$n(\lambda) = A + \frac{B}{\lambda^2} + \frac{C}{\lambda^4} \quad (4.3)$$

Where n is the refractive index, λ is the wavelength of the light and A , B and C are coefficients.

The backside correction option has to be switched on, because the substrate is transparent and therefore the light can get reflected at the backside of the substrate. Then the layer thickness is set to 1 mm and the number of back reflections turned to a fit parameter. Further settings have to be activated:

- Multi Sample Analysis: since several samples should be fitted together.
- Transmission Data Weighting: set to 1000%, since the SE data have two sets (Ψ and Δ) for seven angles (between 45° and 75°), and the transmission data has only one.
- Include Depolarization Data: set to 100%, since the backside reflection that occurs on the bottom side of the glass, is incoherent now.

The "Multi Sample Analysis", abbreviated by MSA, can be found in the Model Options chapter. Here, the two MSA parameters, number of back reflections and thickness can be added, if their fit option has been turned on before.

Fitting Process

After that, the transparent region of the substrate has to be selected. This can be achieved by selecting the measurement file of the transmission measurement, where the transparent part can be seen easily. This is the part, where most of the light is transmitted, so the transmission intensity is approximately 90%. This region is on the higher wavelength side of the graph and ends, when the curve suddenly drops down towards the lower wavelengths. The selected region will then be displayed in the graph, and should now be a more or less flat curve. After that, the first fit can be done. In this step, the three sets of parameters that have to be determined (n , k and the thickness of each measurement) are reduced to just two

parameters, since the extinction coefficient k is zero in the transparent region. Furthermore, the utilization of the MSA for the simultaneous analysis of all samples simplifies the set of parameters, by reducing the number of remaining n to just one. This is because all samples must share the same value for n , leaving only the thickness as the variable across all samples. After this fit, only the transparent region is covered. To evaluate the sample characteristics of the whole spectrum, the Cauchy layer now has to be converted to a B-Spline, with a node resolution of 0.3 eV . The program will continue the fit process by performing a wavelength expansion.

Saving the Material

As the substrate is the bottom layer of every sample, its model characteristics should be applied for all following sample fits. Therefore the finished model should be saved as a material, so it can be used for all remaining samples to simulate the substrate.

4.2 Polymer Layer

Model Building

Now the samples with the semiconductor layer can be evaluated. The measurement files have to be loaded in the program as mentioned in the previous section, but of course, the files of one specific series of a polymer have to be chosen now. This time, the sample consists of two layers, which is the glass substrate with the polymer layer on top of it. The model in the program must therefore be built the same way, with the glass substrate layer as the saved material now and the polymer layer added on top of it, which is again, a Cauchy layer. Subsequently, the remaining settings, mentioned in the section “Glass Substrate Layer and General Evaluation Process”, have to be done, starting from the paragraph “Model Building and Presets” without the step of saving the model. There are small changes this time: the node resolution of the polymer layer should be 0.1 eV now, but this time it will not be able to fulfill this. Instead the resolution will be higher and can be changed afterwards. The important difference here is, that the thickness must be added as a fit parameter in the layer and in the MSA as well.

Further Fitting of the Sample

Following this first fit of the model, some settings of the B-Spline have to be changed right away, before fitting it again. The resolution should be changed to 0.1 eV , if it was not that high during the wavelength expansion fit. The Infrared Amplitude (abbreviated as “IR Amp”) must be changed to zero in addition to turning off the fit option. The B-Spline preset will assume a band gap, which must be turned off. Now the transparent region can be set. It is recommended to set the transparent region starting from the point of the longest wavelength, when the curve drops significantly into the first intransparent region, and ending in the far infrared region, which is $10\,000 \text{ nm}$.

After the fit process, if the following parameters have been significantly altered, they must be corrected. The Epsilon Infinity, abbreviated as “E Inf” should tend to be 1. The parameters of the Multi Sample Analysis chart should stay in a meaningful range, which means, the thicknesses should range between about 10 nm and 100 nm and the number of back reflections should be between 0.5 and 2, except the ones of the transmission measurements, that were set to 0 on purpose. If the values deviate significantly from the expected range, they should be reset to appropriate values, and the model can be fitted again.

Anisotropy and Roughness

Once the previous steps are done, the model simulated in the program is isotropic and does not show any characteristics of roughness. Since this would be an ideal model, and the real sample will not show these ideal characteristics, the following two options were included.

Anisotropy, as explained in the chapter “Physical Background”, describes the structural property of the medium, to behave differently, when the electric field of the light is orientated differently. In this part of the program the anisotropy that is simulated, is only the one in the x-z-plane. In this case, the x-y-direction is the one that is along the interfaces and the z-direction is perpendicular to them. This means there are two sets of optical constants:

The ordinary optical constants are the ones in the x-y-direction, which can be determined much better. This is the case, because the incoming light beam can be separated into 2 components, as mentioned in a previous chapter. The s-polarized light beam is only oscillating in the x-y-direction of the medium and can therefore only be used to determine the optical constants in this direction. But the p-polarized light beam is oscillating in both, the z-direction, and the x-y-direction too. This is because the light beam is not orientated

parallel to the interface, but has an incidence angle of somewhere between 45 and 75 degrees, so a part of the p-polarized light beam is oscillating in the x-y-direction, and only the remaining part can be used to determine the so called “extraordinary optical constants”, of the z-direction.

The transmission intensity measurement is also only influenced by the x-y-oscillations, meaning that the in-plane parameter E_x is fitted by the transmission intensity data and the standard ellipsometry data. Since the SE data is influenced partially by the z-direction, the data seems “noisy”. This “noise” is then used to fit the out-of-plane, so the E_z component.

The **roughness** of the real sample is simulated by an additional “roughness layer” on top of the actual polymer layer. The roughness layer is a mixture of 50% polymer material and 50% air. This option was only used at the evaluation of MDMO-PPV. Most of the time the “Roughness” option did not achieve a significantly lower MSE, but “Anisotropy” did. The isotropic B-Spline should therefore be converted to anisotropic. Since, as explained, the extraordinary optical constants can be determined worse, the resolution of E_z should be set to 0.2 eV, and then fit again.

The next step is to increase the resolution of E_x in wavelength regions, where the model curve shows a strong difference to the measured curve. Most of the time this region will be somewhere between 400 and 700 nm, where the first drop of the transmission intensity occurs. The differences between those curves in the UV region will not be able to be corrected, since they appear because of an insufficient fit accuracy of the glass substrate. The node interval can be decreased in the selected region down to 0.02 eV.

Fitting All Measurements of All Polymers

After each series of all samples were fitted individually, the whole set of measurements from one specific sample can be fit together. Then the optical constants can be compared by these multi sample analysis fits, and they should not show significant differences. The extraordinary constants are once again not as important as the ordinary ones. To check the quality of the fits, the thicknesses can be compared as well. But it is important to only compare the thicknesses of one and the same sample. For instance, if there are two samples available with the same processing speed, these two samples do not have to be fitted with a similar thickness. Instead a particular sample should be fitted with similar thicknesses in both, the series-wise multi sample analysis fit and the combined one too.

4.3 Evaluated Measurements

All sample batches were measured separately after manufacturing them in the order of the series numbers, except for the 3rd series, which was measured together with the 2nd one. Within every measurement series, all samples of a polymer were measured sequentially in the standard ellipsometry mode, starting from the slowest blading speed and progressing to the fastest one, before the samples of the next polymer were measured in the same order. Then the sample holder was changed, and the samples were again measured in the same order. The measured data was then, as explained before, initially evaluated individually, and thereafter collectively. Subsequently, in the next section, the results were based only on the combined data. A detailed description for each polymer of the measurement files, that was taken into account for the evaluation, the activated fit parameters, as well as the final MSE can be seen in the following list:

- **F8BT**

Here, the combination of both series did not achieve a good enough result. So the two individual complex refractive indices of each evaluation were used to subsequently calculate the average of both. For the 1st series, there were 3 to 5 measurements made at different positions and varying azimuthal orientations in 45° steps. This was done because, at the beginning, in-plane anisotropy could not be ruled out. However, it turned out that it did not occur in a significant amount, but the film thickness was slightly inhomogeneous. For each position measured in the SE mode the transmission was measured as well. Then all measurement data sets (N=17) were fitted jointly in a Multi Sample Analysis, the layer thickness (See the first three rows of Table 4.1) and the backside reflection were individual fit parameters, and the overall MSE was 3.8. For the 2nd series, there were only two SE measurements and one transmission measurement done for each sample, so all data sets (N=9) were fitted jointly in an MSA and the layer thickness (See the last three rows in Table 4.1) and the backside reflection were individual fit parameters again. The overall MSE was 4.7.

- **MDMO-PPV**

This polymer was measured and evaluated only in the 4th series with 3 to 4 SE measurements on different positions and with varying azimuthal orientations and one transmission measurement for each sample. All measurement data sets (N=13) were fitted jointly in an MSA, the layer thickness (See Table 4.2) and the backside reflections were individual fit parameters, and a common surface roughness layer was added (4.2 *nm*). The overall MSE was 6.6.

- **PDCBT**

All three measurement series could be combined here, but while all the files of the 2nd and 3rd series could be used, only the transmission files of the 1st series could be used for the evaluation. Subsequently all data sets (N=16) were fitted jointly in an MSA, the layer thickness (See Table 4.3) and the backside reflection were individual fit parameters, and the overall MSE was 5.9.

- **PTB7**

Every sample of both measurement series was measured two times at different positions in 0 and 90° azimuthal orientation (except for the 10 *mm/s* sample of the 1st series, which was measured a third time in 45° orientation) and once in the transmission mode. Then all measurement data sets (N=22) were fitted jointly in an MSA, the layer thickness (See Table 4.4) and the backside reflection were individual fit parameters, and the overall MSE was 5.3.

- **PBDB-T-2F**

Here, the samples were only produced in the 4th series and were measured in the SE mode 2 to 8 times, since the 10 *mm/s* and the 15 *mm/s* sample showed a slight in-plane anisotropic behavior at first glance. However, it was revealed in the evaluation, that this was not the case after all. Every position that was measured in the SE mode, was then also measured in the transmission mode. All data sets (N=23) were fitted jointly in an MSA, the layer thickness (SEE Table 4.5) and the backside reflection were individual fit parameters, and the overall MSE was 9.9.

- **ZZ50**

For this polymer, all samples of both series were measured two times on different positions in 0 and 90° azimuthal orientation (except for the 10 *mm/s* sample of the 2nd series, which was measured a third time in 45° orientation) and once in the transmission mode. Then all measurement data sets (N=19) were fitted jointly in an MSA. The layer thickness (SEE Table 4.6) and the backside reflection were individual fit parameters, and the overall MSE was 7.7.

4.4 Results

4.4.1 Thicknesses

In addition to the complex refractive index, the ellipsometry data evaluation fitted the thickness of each polymer layer. The results of all polymers can then be compared to the profilometry results of each sample. In the following tables, these data are compared for each polymer separately.

The polymer of each table can be seen in the caption. In the first column, the series number can be seen, followed by the doctor blading speed (v_{DB}), the calculated thickness of the ellipsometry evaluation (d_{SE}) with the corresponding standard deviation, and the measured thickness of the profilometer (d_P) with the corresponding standard deviation, are shown in the table as well as the comparison of both thickness values.

Table 4.1: Thickness Table of F8BT

Series	v_{DB} in mm/s	d_{SE} in nm	d_P in nm	d_P in % of d_{SE}
1	2.5	10.0 ± 1.3	7 ± 2	70
1	5	20.8 ± 2.1	12 ± 8	58
1	10	29.0 ± 1.2	17 ± 5	59
2	10	40.5 ± 0.9	34 ± 4	84
2	20	61.1 ± 1.1	50 ± 5	82
2	30	74.2 ± 1.7	71 ± 5	96

Table 4.2: Thickness Table of MDMO-PPV

Series	v_{DB} in mm/s	d_{SE} in nm	d_P in nm	d_P in % of d_{SE}
4	5	51 ± 5	40 ± 6	78
4	10	94.7 ± 2.8	82 ± 7	87
4	15	115.5 ± 1.4	104 ± 9	90

Table 4.3: Thickness Table of PDCBT

Series	v_{DB} in mm/s	d_{SE} in nm	d_P in nm	d_P in % of d_{SE}
1	2.5	8.3 ± 0.9	8 ± 4	96
1	5	9.4 ± 1.0	8 ± 1	85
1	10	21.0 ± 2.1	15 ± 2	71
2	10	38.1 ± 0.5	23 ± 7	60
2	20	58 ± 2	51 ± 8	88
2	30	81 ± 2	66 ± 8	81
3	10	26.2 ± 0.7	24 ± 3	92
3	20	84.0 ± 1.1	75 ± 6	89

Table 4.4: Thickness Table of PTB7

Series	v_{DB} in mm/s	d_{SE} in nm	d_P in nm	d_P in % of d_{SE}
1	2.5	5.17 ± 0.21	5 ± 3	97
1	5	9.1 ± 0.2	6 ± 3	66
1	10	16.2 ± 1.3	14 ± 4	86
4	10	17.7 ± 1.5	14 ± 4	79
4	15	25.9 ± 1.6	18 ± 5	69
4	25	35.7 ± 2.2	26 ± 4	73
4	35	43.6 ± 1.8	42 ± 5	96

Table 4.5: Thickness Table of PBDB-T-2F

Series	v_{DB} in mm/s	d_{SE} in nm	d_P in nm	d_P in % of d_{SE}
4	10	32.2 ± 2.3	24 ± 2	75
4	15	50.1 ± 2.6	41 ± 4	82
4	20	51.6 ± 0.7	36 ± 4	70
4	30	62 ± 4	51 ± 5	82

Table 4.6: Thickness Table of ZZ50

Series	v_{DB} in mm/s	d_{SE} in nm	d_P in nm	d_P in % of d_{SE}
0	2.5	15.3 ± 0.8	15 ± 2	98
0	5	19.9 ± 0.4	18 ± 2	90
0	10	23.6 ± 0.7	25 ± 3	106
2	10	22.7 ± 0.4	31 ± 6	137
2	20	37.7 ± 2.3	43 ± 2	114
2	40	62 ± 5	62 ± 3	100

4.4.2 Complex Refractive Indices

Once the whole fitting process is done, all components of the resulting complex refractive index can be seen in the program. The components, n and k , for the ordinary and the extraordinary direction of all polymers are shown in Figure 4.1.

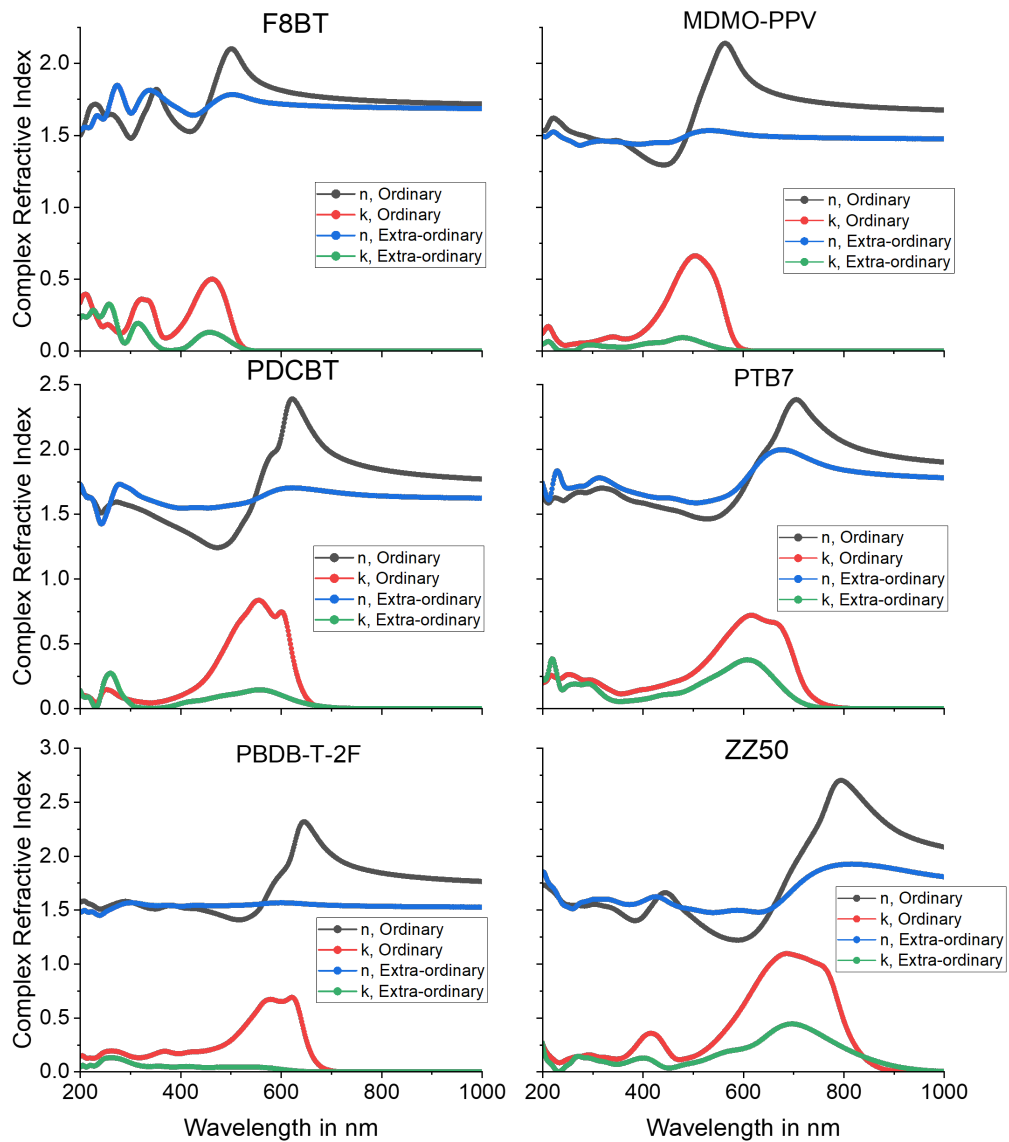


Figure 4.1: n and k of all Polymers

5 Absorption Coefficient and Energy Gap

The remaining part is to evaluate the absorption coefficient, the first peak of the absorption coefficient at the lowest energy (hereinafter referred to as absorption maximum with its corresponding peak energy) and the energy gap, calculated by the Tauc Plot method. [4]

5.1 Absorption Coefficient

The absorption coefficient α was calculated with the formula (2.3). Here, only the ordinary part of the extinction coefficient k was used to determine α . Figure 5.1 shows the plots for the absorption coefficients for the analyzed polymers.

After that, the aim was to determine the absorption maximum, so the first peak on the left-hand side of the plot. In the case of MDMO-PPV, PTB7 and ZZ50 this is not a full peak, but a small shoulder on the left side of the bigger peak. The relation between the peak value and its energy value were then plotted in the Figure 5.2. The dots of the corresponding polymers were color-coded to match the colors of the polymer layers of the samples.

All first transition peaks of the analyzed samples were in the visual range (The wavelength range of 400 - 800 nm correspond to the energy range 3.1 - 1.55 eV). It seems, that there is no correlation between the absorption coefficient and the corresponding energy values.

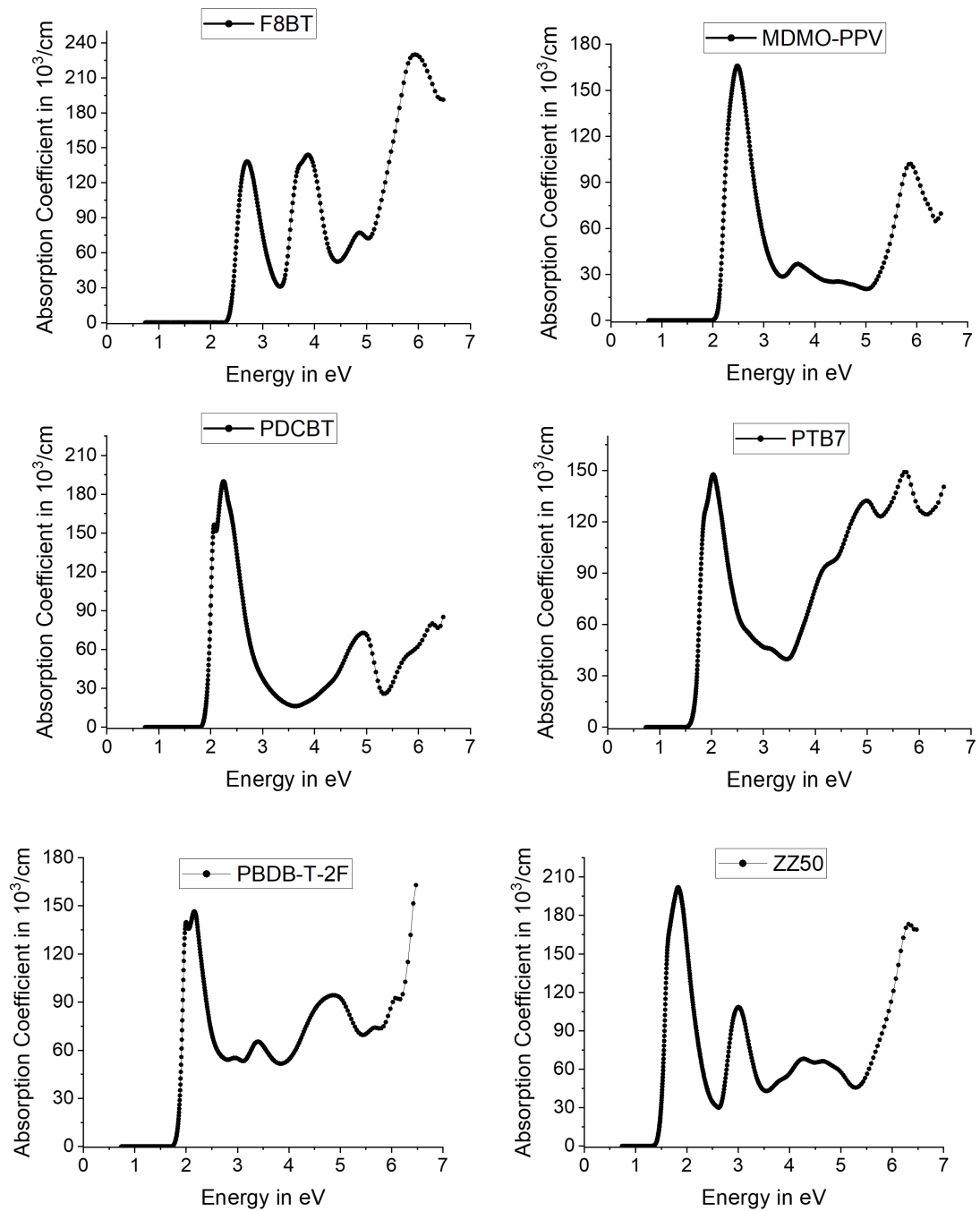


Figure 5.1: Absorption Coefficients of All Polymers

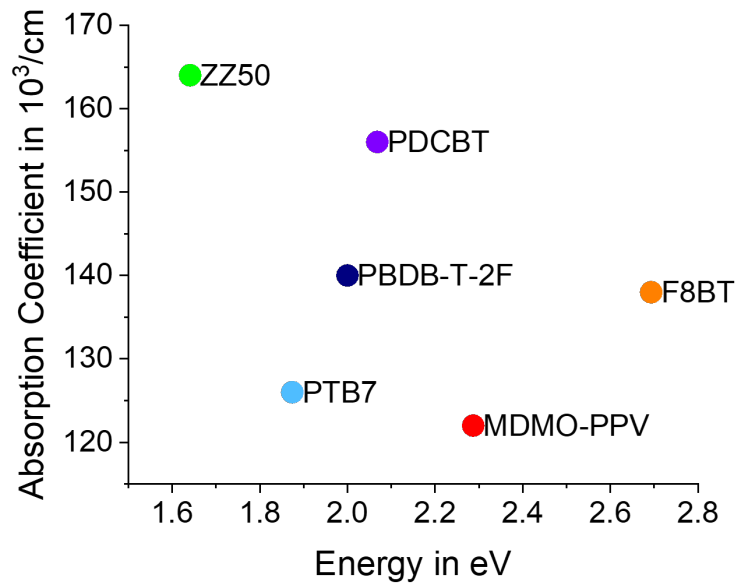


Figure 5.2: First Transition Peaks as a Function of the Energy

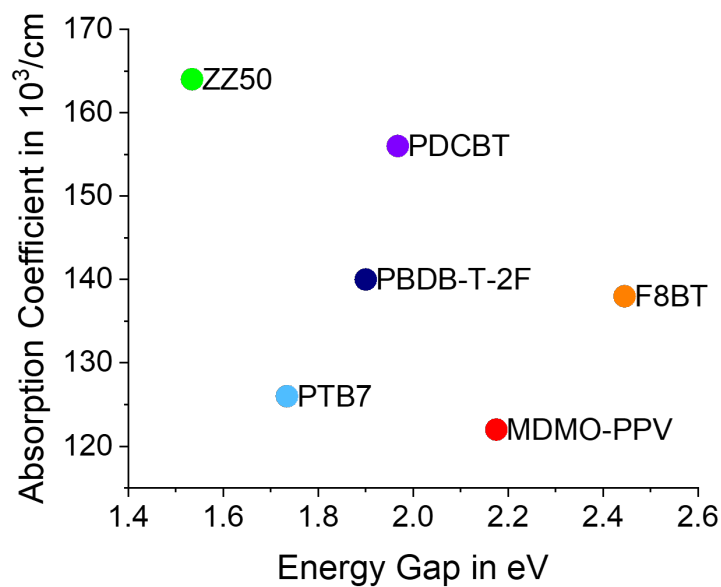


Figure 5.3: First Transition Peaks as a Function of the Energy Gap

5.2 Tauc Plot and Energy Gap

The functions of the polymers' absorption coefficients α are then needed for the Tauc Plot. The Tauc Plot is used to determine the optical energy gap of semiconductors and is based on equation (5.1) [4]

$$(\alpha \cdot h\nu)^{1/\gamma} = B(h\nu - E_g) \quad (5.1)$$

Where α is the absorption coefficient, $h\nu$ is the photon energy, E_g is the energy gap and B is a slope. The factor γ depends on the type of electronic transition. In the case of the analyzed polymers, γ is always 1/2, so the exponent will be 2.

The left part of the equation (5.1) then has to be calculated and plotted as a function of the photon energy. After that the increase of the first peak is fitted with a Linear Fit, which is the line, that is described by the right part of the equation. All polymers together are plotted in Figure 5.4. Here, only the first peak is shown in the plots, so the energy scale is only shown between approximately 1.5 eV and 3 eV.

The zero of the function E_g is the calculated energy gap of the polymer. All the energy gaps of every evaluation series are then combined and shown in Figure 5.5 and in Table 5.1. The errors have been derived through estimation, utilizing the MSE values of the ellipsometry fits as a basis for their determination. The circles represent the literature values for comparison.

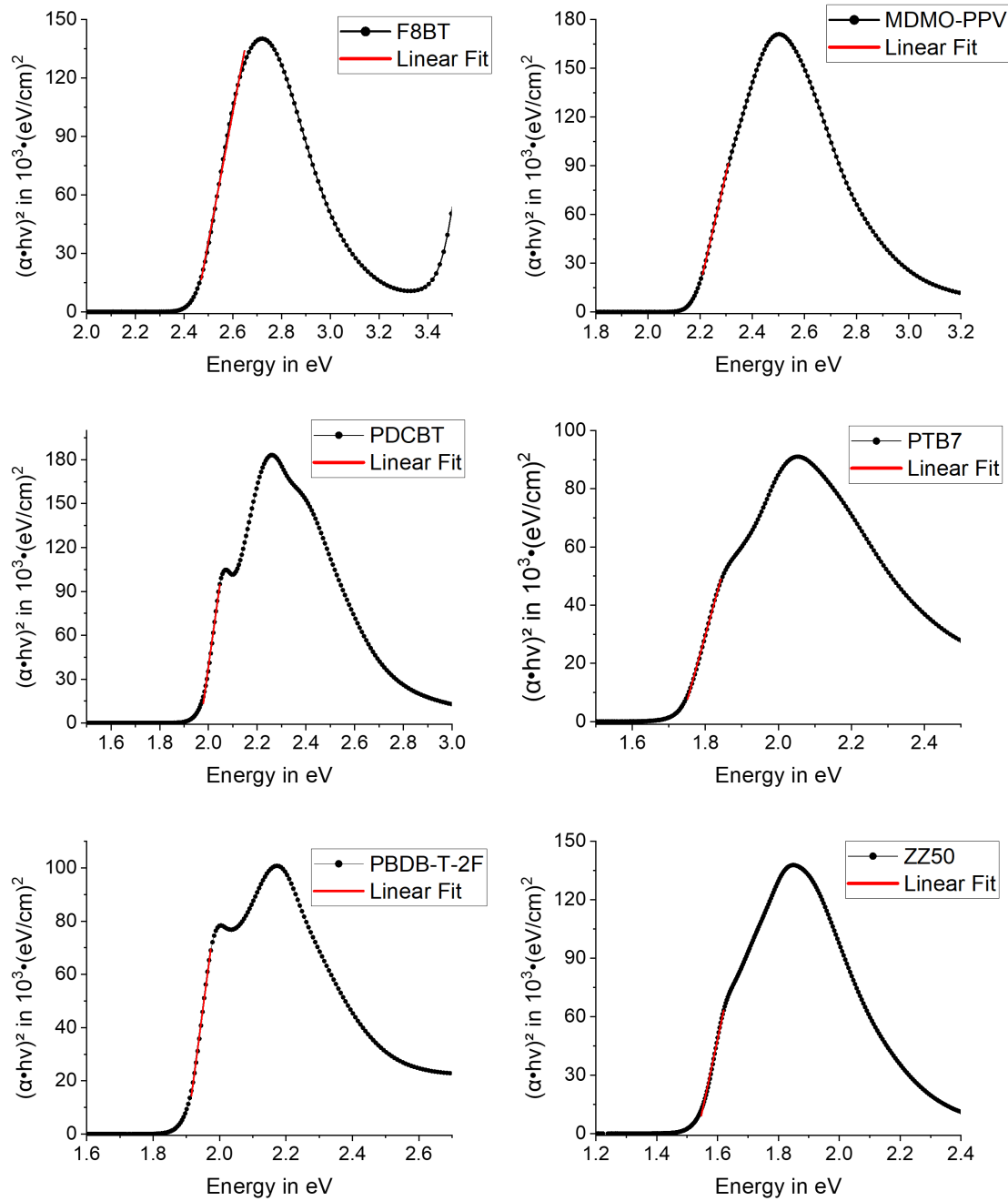


Figure 5.4: Tauc Plot and Linear Fit of All Polymers

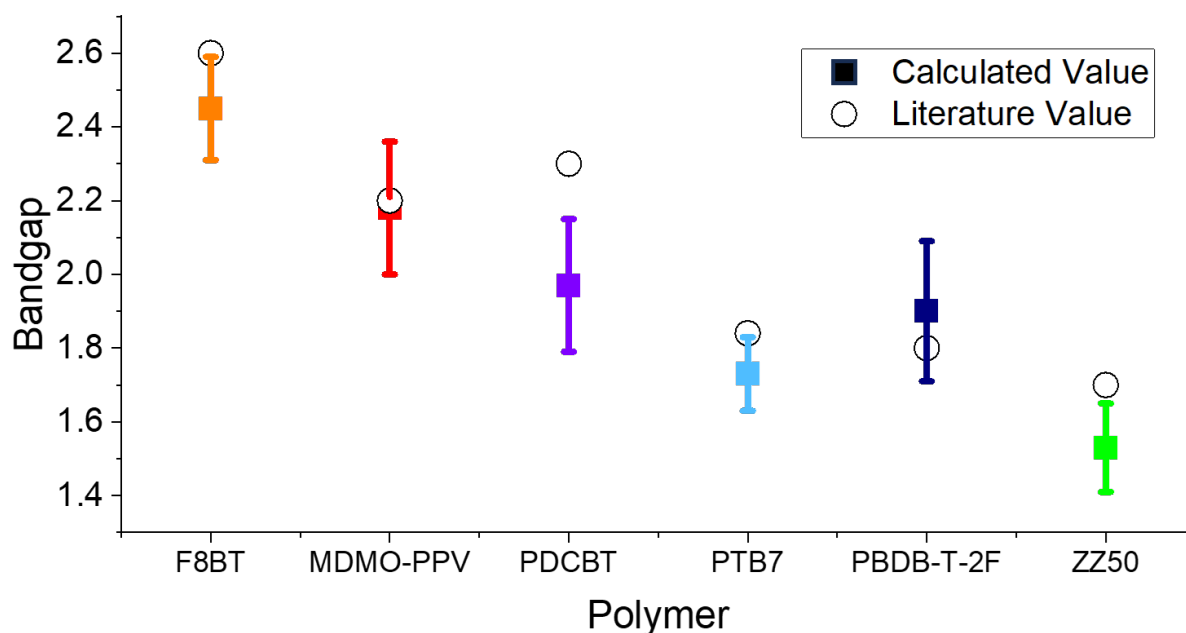


Figure 5.5: Energy Gaps of the Evaluated Series

Polymer	$E_{g,calc}$ in eV	$E_{g,Lit}$ in eV
F8BT	2.45 ± 0.14	2.6 [5]
MDMO-PPV	2.18 ± 0.18	2.2 [11]
PDCBT	1.97 ± 0.18	2.26 [8]
PTB7	1.73 ± 0.10	1.84 [12]
PBDB-T-2F	1.90 ± 0.19	1.8 [6]
ZZ50	1.53 ± 0.12	1.7 [7]

Table 5.1: Calculated Energy Gap Compared to Literature Values

In all cases, literature values were provided for the HOMO and LUMO levels, and the term “energy gap”, as used here, refers to the HOMO/LUMO gap, which was subsequently calculated. Out of the six calculated values, only two fall within the first confidence interval of the literature values, with two others just slightly outside by 0.01 eV. The remaining two are within the second confidence interval. After calculating the energy gap with the Tauc Plot method, the peak values of the absorption coefficient can be plotted in relation to the energy gap values, which can be seen in Figure 5.3

The position of the dots did not differ significantly from the ones of the previous absorption coefficient plot (5.2). Thus there is also no correlation between the absorption coefficient and energy gap visible.

Since the two plots look very similar, the energy gap values (E_g) and the energy values of each absorption peak (E_P) were compared. Interestingly, those two values show a relation for the analyzed polymers, as it is shown in table 5.2

Polymer	E_P in eV	E_g in eV	Deviation in %
F8BT	2.69	2.45	9.8 ± 0.9
MDMO-PPV	2.29	2.18	5.0 ± 1.9
PDCBT	2.07	1.97	5.1 ± 1.1
PTB7	1.87	1.73	8.1 ± 2.4
PBDB-T-2F	2.00	1.90	5.3 ± 1.1
ZZ50	1.64	1.53	7.2 ± 2.7

Table 5.2: Relation Between the Energy Gap and the Peak Energy

The deviation tends to be in the range between approximately 5 and 10 %. The weighted arithmetic mean of the deviation is 7.4 ± 2.1 %. It was calculated as follows: Both, the energy gap and the peak energy value cannot be measured and calculated exactly, so the calculated values deviate from the actual ones in the order of approximately $0.1 eV$. But the relation of the calculated values to each other can be determined more precisely. This can easily be seen by the fact, that the calculated energy gap must always be smaller than the peak energy, since the energy gap represents the increase of the peak, which cannot be located after it. The calculated energy gap was easy to determine, but the peak energy was more difficult, particularly for the cases, in which the peak energy was located in the shoulder (estimated error: $0.4 eV$) and not in the full peak (estimated error: $0.2 eV$). The errors of the deviations were therefore based on the estimated precision of each peak energy.

6 Summary

Initially, it posed a challenge to determine the precise location of the first peak, particularly in the cases where it overlapped the bigger full peak. This led to more uncertainty of the determination of both the absorption maximum and the peak energy value of the affected polymers. However, once the linear fits of the Tauc plots were performed, the task of identifying the exact peak energy value became more manageable, as it has to be slightly higher than the highest energy value still included in the linear fit. The only polymer that remained difficult to examine was MDMO-PPV, where first peak is almost completely overlapped by a higher full peak.

Nevertheless, both plots (5.2 and 5.3) revealed no discernible correlation between the plotted values. In fact, the three polymers ZZ50, PDCBT and F8BT appeared to align along a straight line, which may represent the upper boundary for the relation between the absorption maximum and both the peak energy and the energy gap. However, for a more accurate understanding of these relationships, it would be necessary to analyze more polymers, especially in the high energy range. Additionally it would also be interesting if there are more polymers with similar energy gap, but differing absorption maxima, such as in the case of PDCBT and PBDB-T-2F.

An interesting observation emerged regarding the relationship between the peak energy and the energy gap of each polymer. The peak energy tended to be approximately 5 to 10 % higher than the energy gap. This means, that the width of the curve increases as the energy gap and, consequently, the peak energy rise. Therefore, within the analyzed set of polymers, the curve width of the first peak primarily depends on its position on the energy spectrum, and seems to not be affected by the absorption maximum. Once again, an analysis involving more polymers would be required for a more in-depth examination of this relationship.

List of Figures

2.1	Bandgap Explanation	4
2.2	HOMO/LUMO gap [14]	4
2.3	Effect of Anisotropy: The two perpendicular components E_x and E_z of the electric field of a light beam are both propagating along the y-axis, but influenced differently when traveling through the anisotropic material	5
2.4	Angle of Incidence: The incoming (I), the reflected (R) and the transmitted (T) ray and their angles are shown	6
2.5	The incoming light ray gets reflected and transmitted at each interface. A part of it gets absorbed while traveling through the media.	8
2.6	The s-polarized (s) and p-polarized part (p) of the reflected beam cause the tilt Ψ . The incoming light beam (L) was linearly polarized	10
2.7	When the light is linearly polarized, the s-component and the p-component are in phase ($\Delta = 0$). Once the beam gets reflected, the two polarization components are out of phase (phase shift Δ), causing an elliptical polarization.	10
3.1	F8BT	11
3.2	MDMO-PPV	11
3.3	PDCBT	11
3.4	PTB7	12
3.5	PBDB-T-2F	12
3.6	ZZ50	12
3.7	Complex Refractive Indices of Both Sides of the Glass	13
3.8	Some Labeled Samples of Each Polymer with Different Blading Speeds	16
3.9	Ellipsometry Measurement Modes	17
3.10	Ellipsometer Woollam M2000 [3]	17
4.1	n and k of all Polymers	32
5.1	Absorption Coefficients of All Polymers	34
5.2	First Transition Peaks as a Function of the Energy	35
5.3	First Transition Peaks as a Function of the Energy Gap	35

5.4	Tauc Plot and Linear Fit of All Polymers	37
5.5	Energy Gaps of the Evaluated Series	38

List of Tables

4.1	Thickness Table of F8BT	30
4.2	Thickness Table of MDMO-PPV	30
4.3	Thickness Table of PDCBT	30
4.4	Thickness Table of PTB7	30
4.5	Thickness Table of PBDB-T-2F	31
4.6	Thickness Table of ZZ50	31
5.1	Calculated Energy Gap Compared to Literature Values	38
5.2	Relation Between the Energy Gap and the Peak Energy	39

Bibliography

- [1] J. V. CASPAR and T. J. MEYER, “Application of the Energy Gap Law to Nonradiative, Excited-State Decay,” *The Journal of Physical Chemistry*, vol. 87, no. 6, pp. 952–957, 1983.
- [2] J. A. WOOLLAM CO., *CompleteEASE Software Manual*, Written for CompleteEASE 6.54, Equation 3-1.
- [3] J. A. WOOLLAM CO., *M-2000 Ellipsometer*. [Online]. Available: <https://www.jawollam.com/products/m-2000-ellipsometer> (visited on 2023-10-17).
- [4] P. MAKUŁA, M. PACIA, and W. MACYK, “How to correctly determine the band gap energy of modified semiconductor photocatalysts based on uv–vis spectra,” *The Journal of Physical Chemistry Letters*, vol. 9, no. 23, pp. 6814–6817, 2018. DOI: 10.1021/acs.jpcllett.8b02892. eprint: <https://doi.org/10.1021/acs.jpcllett.8b02892>. [Online]. Available: <https://doi.org/10.1021/acs.jpcllett.8b02892>.
- [5] OSSILA, *F8BT (PFBT)*. [Online]. Available: <https://www.ossila.com/products/f8bt> (visited on 2023-10-19).
- [6] OSSILA, *PBDB-T-2F (PM6)*. [Online]. Available: <https://www.ossila.com/products/pbdb-t-2f> (visited on 2023-10-19).
- [7] OSSILA, *PCPDTBT*. [Online]. Available: <https://www.ossila.com/products/pcpdtbt> (visited on 2023-10-19).
- [8] OSSILA, *PDCBT*. [Online]. Available: <https://www.ossila.com/products/pdcbt> (visited on 2023-10-19).
- [9] OSSILA, *PTB7*. [Online]. Available: <https://www.ossila.com/products/ptb7> (visited on 2023-10-19).
- [10] OSSILA, *Solution Coating Methods: A Comparison*, Paragraph: Doctor Blading. [Online]. Available: <https://www.ossila.com/pages/solution-processing-techniques-comparison> (visited on 2023-10-19).
- [11] SIGMA-ALDRICH, *Poly-[5-(3',7'-dimethyloctyloxy)-2-methoxy-1,4-phenylenvinylen]*. [Online]. Available: https://www.sigmaaldrich.com/AT/de/product/aldrich/546461?gclid=CjwKCAjw7c2pBhAZEiwA88p0F5ovUY0b8gLLMn19vtPHTUTXJacLIpb2tb3beTWaCaL_W3XmkdZaYRoCSQIQAvD_BwE (visited on 2023-10-19).

- [12] SIGMA-ALDRICH, *PTB7*. [Online]. Available: <https://www.sigmaaldrich.com/AT/de/product/aldrich/772410> (visited on 2023-10-19).
- [13] K. STELLMACH, *What can organic solar cells bring to the table?* [Online]. Available: <https://www.greenbiz.com/article/what-can-organic-solar-cells-bring-table> (visited on 2023-10-23).
- [14] UNIVERSITY OF CAMBRIDGE, *Organic Semiconductors*. [Online]. Available: <https://www.oe.phy.cam.ac.uk/research/materials/osemiconductors> (visited on 2023-10-18).